3D Localization of RFID Tags with a Single Antenna by a Moving Robot and "Phase ReLock"

Anastasios Tzitzis, Spyros Megalou, Stavroula Siachalou, Emmanouil Tsardoulias, Traianos Yioultsis, Antonis G. Dimitriou
School of Electrical and Computer Engineering
Aristotle University of Thessaloniki
Thessaloniki, Greece
antodimi@ece.auth.gr

***Abstract*—In this paper, we propose a novel method for the three dimensional (3D) localization of RFID tags, by deploying a single RFID antenna on a robotic platform. The constructed robot is capable of performing Simultaneous Localization (of its own position) and Mapping (SLAM) of the environment and then locating the tags around its path. The proposed method exploits the unwrapped measured phase of the backscattered signal, in such manner that the localization problem can be solved rapidly by standard optimization methods. Three dimensional solution is accomplished with a single antenna on top of the robot, by forcing the robot to traverse non-straight paths (e.g. s-shaped) along the environment. It is proven theoretically and experimentally that any non-straight path reduces the locus of possible solutions to only two points along the 3D space, instead of the circle that represents the corresponding locus for typical straight robot trajectories. As a consequence, by applying our proposed method "Phase Relock" along the known half-plane of the search-space, the unique solution is rapidly found. We experimentally compare our method against the "holographic" method, which represents the accuracy benchmark in prior-art, deploying commercial off-the-shelf (COTS) equipment. Both algorithms find the unique solution, as expected. Furthermore, "Phase ReLock" overcomes the calculations-grid constraints of the latter. Thus, better accuracy is achieved, while, more importantly, Phase-Relock is orders of magnitude faster, allowing for the applicability of the method in real-time inventorying and localization.**

***Index Terms*—RFID, 3D Localization, Phase Unwrapping, Non Linear Optimization, Robotics, SLAM**

I. Introduction

This work is part of a research project [1] and focuses on automatic real-time inventorying and localization, in applications such as libraries, retail stores, warehouses, etc. All target objects are "tagged" with a passive RFID tag. Currently, the most common RFID tag costs about 0.1$. As a result, its deployment on almost any object is feasible, since it does not increase its market value. Furthermore, in contrast to "traditional" approaches based on barcode technology, RFID technology offers larger reading rate without demanding visual contact. It also liberates manual inventorying, usually associated with errors and delays.

This research has been cofinanced by the European Union and Greek national funds through the Operational Program Competitiveness, Entrepreneurship and Innovation, under the call RESEARCH CREATE INNOVATE (project code:T1EDK-03032).

Although localization of RFID tags tends to become a well-studied domain, most of the research has been focused on the 2D problem. Localization in 3D has been proved a quite challenging task. Most of the proposed 3D methods demand the installation of multiple readers and antennas to cover the space of interest [2]- [4]. The more the deployed antennas, the better the expected accuracy. The cost of such fixed installations, though, is huge and therefore, cannot be applied in large environments. As for the "fingerprinting" techniques (i.e. methods that evaluate the unknown position of a target tag based on the similarity of measurements between itself and reference tags) [5]- [7], their accuracy depends on the density of reference tags and the resemblance of the electromagnetic conditions between the reference and the tracked tags. Especially for accurate 3D localization, a pre-deployment of a 3D grid consisted by an extensively large set of reference tags is required. In addition to the above techniques, there are others which deploy a moving antenna that takes measurements along synthetic apertures (SAR) [8]- [12]. For a 3D estimation, they propose that the antenna has to be moved in two perpendicular straight paths. The drawbacks of such methods arise from the fact that they require the manual adjustment of the antenna at a specific position, so it can then move along a second path, at the expense of time and effort.

On the contrary, this work solves the 3D localization problem by using a single antenna, placed on top of a moving robot. A moving robot is capable of covering any space, no matter how large it is. By adjusting its moving strategy, it can collect an infinitely large number of measurements at many closely-spaced antenna locations. For this reason, we have constructed a prototype robotic platform as shown in Fig.1. It can navigate autonomously in unknown environments and perform both SLAM (by optical sensors) and RFID localization. Extending our previous work, [13], we accomplish 3D localization, by forcing the robot to move along non straight trajectories (slalom) while interrogating the tags; this eliminates the circular ambiguity of the possible tag's locations, resulting from straight motion paths. The proposed motion strategy can be applied to any SAR method [8], [12] (also termed as "Virtual Antenna Array" in prior art). In our work, we apply "Phase ReLock", which solves rapidly the problem by standard

Fig. 1. SLAM and RFID enabled robot.

optimization methods. To achieve that, we perform "phase unwrapping" on the measured backscattered phase samples, "correcting" the phases for each tag to take continuous values, instead of being constrained in 2π intervals.

The remainder of the paper is organized as follows: In section II we present the problem. The proposed method is presented in section III. Experimental results and conclusions are given in sections IV and V respectively.

II. Problem Formulation

Consider an antenna moving along a straight trajectory in 3D space, forming an 1-dimensional antenna array $A = [A_1 \ ... \ A_n]$ of successive antenna locations $A_i = (x_i, y_i, z_i)$. A static tag t is placed at (x_t, y_t, z_t). We wish to estimate the 3D position of the tag using the phase of its backscattered signal. The tag's phase measured at A_i is denoted as θ_{it}.

The measured phase is proportional to the round-trip length of the reader-to-tag-to-reader link, plus a constant phase shift, introduced by the deployed hardware. It is also a periodic function with period 2π that repeats every $\lambda/2$, where λ stands for the wavelength of the carrier frequency. The theoretical formula that computes phase is:

$$\phi_{it} = \left(\frac{2\pi}{\lambda} 2d_{it}(x_t, y_t, z_t) + c_t \right) \bmod 2\pi =$$
$$= \left(\frac{4\pi}{\lambda} \sqrt{(x_t - x_i)^2 + (y_t - y_i)^2 + (z_t - z_i)^2} + c_t \right) \bmod 2\pi$$
$$i \in [1, n], \quad (1)$$

where d_{it} represents the Euclidian distance between the tag and the antenna's location A_i. The phase offset c_t is unknown but can assumed identical for every measured sample of the tag, since the same antenna and reader were used for all measurements.

Given a set of phase measurements θ_{it} of the same tag and a set of theoretical values ϕ_{it}, we are looking for the possible tag coordinates for which the two sets best match. For this reason, a proper cost function is necessary to represent the discrepancy of the two sets.

A. Holographic Imaging

In this sense, the state-of-the-art method proposed in [8] and its equivalent [12], create an appropriate cost function. Due to the non convexity of the corresponding functions, the problem can be solved only by an exhaustive search. Therefore, a grid of possible tag locations is necessary and a search on all these locations is performed, to find the one that best matches the measurements. As a result, a "holographic image" is generated, representing the "probability" of each grid-point to be the actual tag location.

The complexity of the image's calculation is proportional to the number of the grid's points. The denser the grid, the higher the expected accuracy and the estimation-time due to exhaustive search. Especially in case of a 3D image, where the number of points is multiplied to the size of the third dimension, the computational burden makes the application of those methods prohibitive.

B. Proposed Method

In order to liberate the localization from a calculation's grid and hence, a time-consuming search, we proposed "Phase ReLock", an earlier version of which treats the two-dimensional problem and can be found in [13]; Phase ReLock is a method that solves the localization problem by unwrapping the phase measurements and applying non linear optimization.

The most frequent optimization problems are solved by the least squared method, which minimizes the following function:

$$F(x_t, y_t, z_t, c_t) = \sum_{i=1}^{n} \left[\phi_{it}(x_t, y_t, z_t, c_t) - \theta_{it} \right]^2 \quad (2)$$

where θ_{it} is the measured phase and ϕ_{it} the theoretical phase computed by (1). In optimization, this problem is usually addressed as fitting a parameterized function (i.e. $\phi_{it}(x_t, y_t, z_t, c_t)$) to a set of measured data (i.e. θ_{it}). We are looking for the unknown parameters (x_t, y_t, z_t, c_t) for which (2) is minimized.

By substituting (1) in (2), a nonlinear cost function is derived. Non linear optimization methods ([14]- [16]) solve the fitting problem by iteratively reducing the value of the cost function. They start from an initial selection of parameters and through a sequence of updates to the parameters' values, they eventually converge to the solution; i.e. in general a cost function's local minimum dependent on the initial point. However, optimization means finding the best solution overall and any optimization method should converge to the global minimum. For this reason, the cost function has to be convex with a distinct global minimum.

III. Phase ReLock

A. Straight Paths

Consider an antenna moving along a straight path and taking measurements from a static tag. A typical curve of the measured phase along the x-coordinate of the antenna, is shown in Fig. 2. As expected, phase is wrapped in $[0, 2\pi]$ intervals, resulting in discontinuities/jumps every 2π. Phase

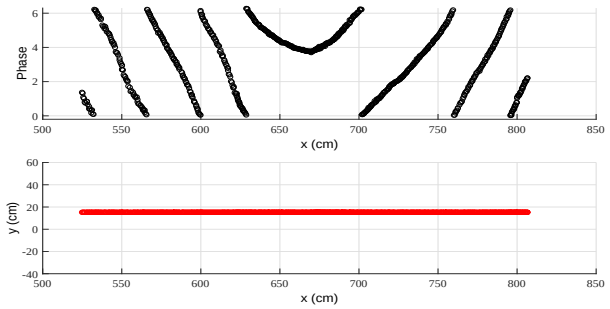

Fig. 2. Measured phase for a static tag (top) - Straight robot's trajectory (bottom)

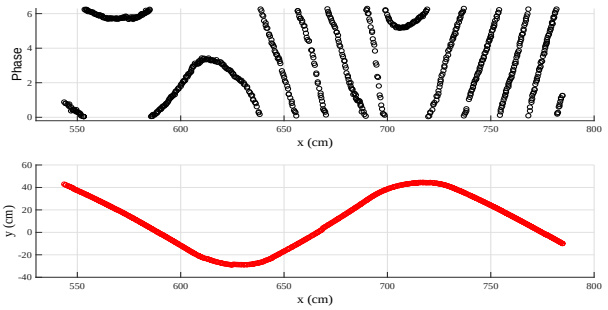

Fig. 4. Measured phase (top) - Non straight robot's trajectory (bottom)

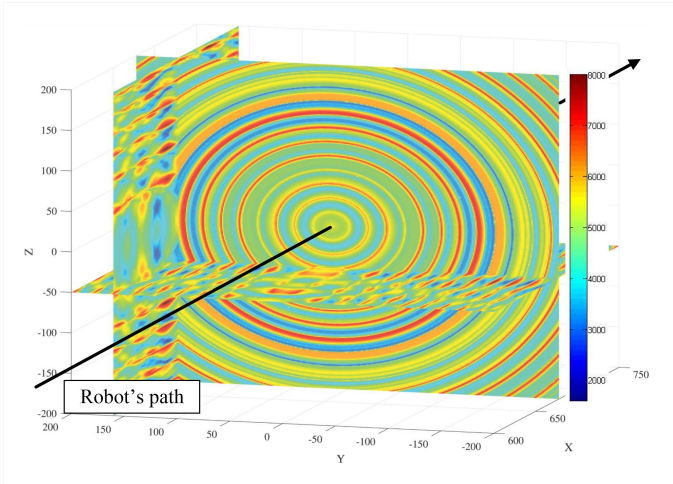

Fig. 3. 3D representation of (2) for a straight robot's path.

also decreases and increases while the tag-to-antenna distance decreases and increases respectively and the curve changes slope ($x_i = 670cm$) when the tag-to-antenna distance is minimum.

Fig. 3 represents the 3D graphical illustration of (2), shown in 2D slices. The slices are through the (incorrectly) estimated tag coordinates $(670, 155, -50)$. Red and blue colors denote high and small amplitudes of (2) respectively; we are interested in the blue color since we are looking for the minimum of (2).

If a *single* antenna moves along a straight path, all points along any circle, located at the plane perpendicular to the antenna's straight path and centered at the point of the trace, where the tag-to-antenna distance is minimized, will have the same distances d_{it} from all antenna locations A_i. Therefore, all such points will result in the same value of (2). Hence, the 3D problem cannot be solved by any method.

This effect is illustrated in the y-z slice at the tag's coordinate $x_k = 670cm$, which indicates the expected rotational symmetry around the antenna array; the points represented by same coloring (i.e. the points corresponding to equal amplitudes of (2)), form circles. The center of all circles is at the antenna location $A_j = (x_j, y_j, z_j)$, where y_j and z_j are the known y and z antenna's coordinates when $x_j = x_k$. As a result, the tag is equally probable to be located anywhere at a fixed distance from A_j (i.e. a circle) in the plane perpendicular to the antenna's array. A theoretical analysis of this effect is provided in the Appendix.

This ambiguity regarding the actual position of the tag would be solved by an additional antenna component in a second dimension. In the Appendix we provide a proof that a second array A', will face this ambiguity and point out only 2 points as the solution of the problem; one in the $z \leq z_i$ half plane and one in $z \geq z_i$, where z_i is the constant height the antenna is placed at. In practice, we can reasonably assume that any non straight antenna's trajectory, such as "slalom", can be approximated as multiple individual straight paths and therefore, solve the 3D localization problem.

B. Non straight Paths

The curve of phase measurements, taken along the non straight trajectory of Fig. 4-bottom is shown in Fig. 4-top. Notice that the curve now changes slope more than once in contrast to the case of a straight path. A local minimum of the phase curve indicates that the tag-to-antenna distance alternates from decreasing to increasing and a local phase maxima indicates the opposite.

Similarly to subsection III-A, the 3D representation of (2) for the phase samples of Fig. 4 is given in Fig. 5. The slices are through the new estimated tag coordinates $(680, 145, -25)$. In comparison with Fig. 3, the circular symmetry of (2) in the y-z slice, has been now eliminated. The points that correspond to lowest values of (2), denoted by intense blue, no longer form a circle, confirming in practice our claim presented in the Appendix.

C. Phase Unwrapping

However, the abrupt changes of color in Fig. 5 indicate the existence of many local minima and maxima. Any optimization algorithm deployed would converge to a local minimum dependent on the initial point, instead of converging to the global one. The non convexity of (2) emerges from the 2π periodicity of both the measured and the theoretical phase computed by (1). Thus, the use of the unwrapped phase, in combination with the removal of the modulus operation in (1) would correct that "abnormal" shape.

The phase unwrapping processing targets to the reconstruction of the phase curve, so that it obtains a continuous form

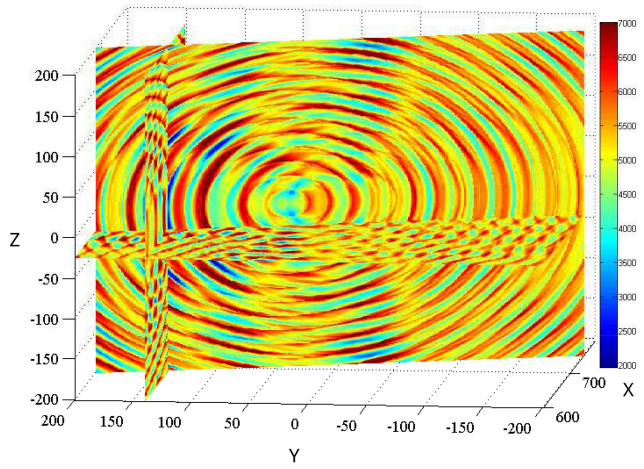

Fig. 5. 3D representation of (2) for a non straight robot's path.

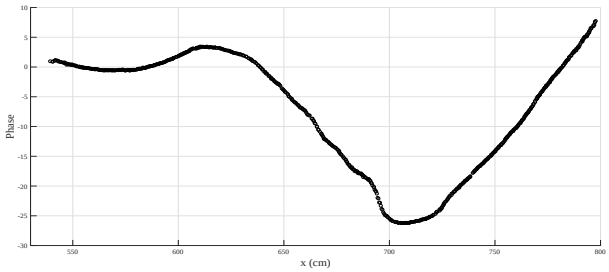

Fig. 6. Unwrapped phase curve.

without any 2π jumps. In [13], a detailed phase unwrapping method is presented. The result of unwrapping the phase curve of Fig. 4-top, is shown in 6.

The modified theoretical function that computes continuous and unwrapped phase values is now given by

$$\phi'_{it}(x_t, y_t, z_t, c_t) = \left(\frac{2\pi}{\lambda} 2d_{it}(x_t, y_t, z_t) + c_t\right) = \\ = \left(\frac{4\pi}{\lambda}\sqrt{(x_t - x_i)^2 + (y_t - y_i)^2 + (z_t - z_i)^2} + c_t\right) \\ i = 1, .., n \quad (3)$$

Similarly, the new cost function is written as:

$$F'(x_t, y_t, z_t, c_t) = \sum_{i=1}^{n} [\phi'_{it}(x_t, y_t, z_t, c_t) - \theta'_{it}]^2 = \\ \sum_{i=1}^{n} \left[\left(\frac{4\pi}{\lambda} d_{it}(x_t, y_t, z_t) + c_t\right) - \theta'_{it}\right]^2 \quad (4)$$

Apart from the constant phase shift introduced by the deployed hardware, the term c_t here also represents the number of whole cycles of phase offset between the unwrapped phase curve and the theoretical one.

Fig. 7 shows that (4) no longer suffers from local minima and its repetitive shape has been "corrected". Since there are two (symmetrical) solutions (see Appendix), there are two

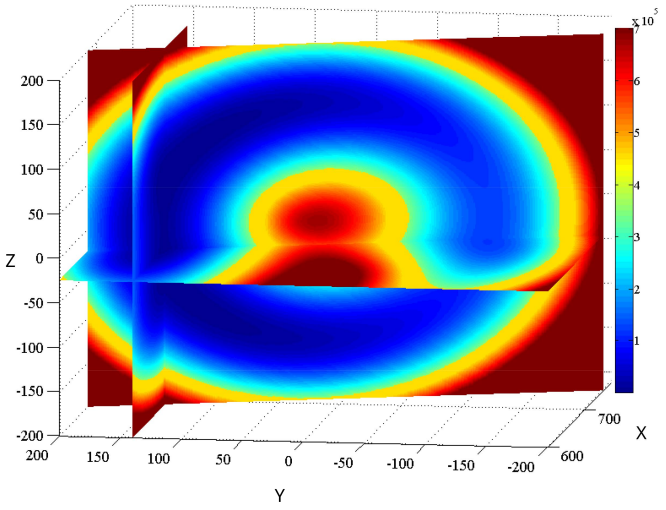

Fig. 7. 3D representation of (4) for a non straight robot's path.

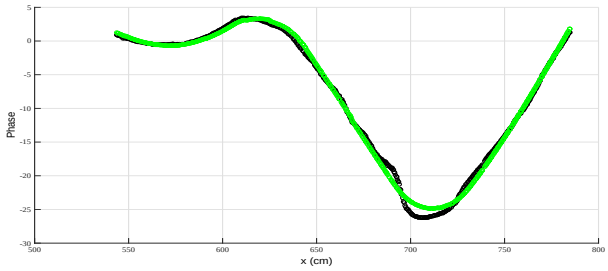

Fig. 8. Unwrapped phase-curve (black) vs. Phase ReLock theoretical curve for the optimum parameters (green).

minima of (4), each of which is global in its half plane. Considering the half plane the tags are located in as known, we can apply an optimization algorithm along the subspace of interest, to minimize (4) and find the optimum parameters (x'_t, y'_t, z'_t, c'_t).

The unwrapped phase curve and the curve produced by (3) for the optimum parameters are compared in Fig. 8. Notice that they mostly coincide, indicating the success of the method.

IV. Experiments

A. Experimental Setup

Experiments were carried out in a corridor-type room inside the Campus, by deploying the custom robot of Fig. 1. The robot is equipped with a combination of sensors to perform SLAM and an antenna and reader to interrogate the RFID tags (refer to [13] for more information). Initially, the robot traverses the a priori unknown environment and creates a map of it, by using SLAM algorithms (e.g. [17]). Then, it moves again through the room in 3 different speeds and slalom-type trajectories to collect measurements from 87 tags, considered to be placed in the half plane $z \geq 0$, assuming that our antenna is placed at $z_i = 0$. Concurrently, the robot continuously estimates its own position in the previously created map. The robot's paths shown in Fig. 9 represent the estimations of

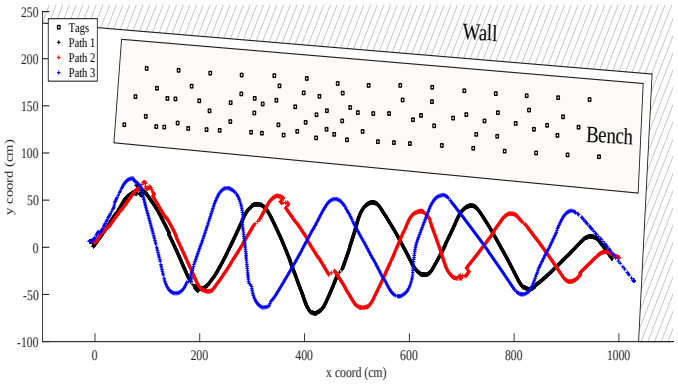

Fig. 9. Trajectories of the robot, as estimated by SLAM.

Fig. 10. Representation of the measurements' set-up.

the SLAM algorithm; the discontinuities/trembling in each trajectory indicate the error of the SLAM algorithm.

B. Evaluation

The average results of Phase Relock for the 3 deployed robot's speeds are given in Table I. The speed seems to be an important aspect of the algorithm, since the total error increases as the robot moves faster and collects fewer phase measurements; best accuracy is achieved at 5cm/s and a mean error of $45cm$ is reported. Notice that the projection of the 3D position on the x-y plane remains same in the 3 experiments, around $17cm$; i.e a value that is in agreement with the 2D results presented in [13].

We compared our proposed method against the holographic methods [8] and [12]. The latter were executed for a $5m \times 2.5m \times 2m$ calculations' grid, with $3cm$ spacing. The average results of the 3 experiments for the 87 tags are compared in Table II. Since the cost functions used in [8] and [12] are equivalent, they have same accuracy, reporting a mean localization error of $58cm$. The mean error for Phase ReLock is slightly better, about $55cm$. It is also recalled that the robot's trace is not known but estimated during SLAM. It is impossible for any SLAM algorithm to compute the robot's pose correctly at all times. Thus, the antenna's coordinates (x_i, y_i, z_i) involved in (4) introduce an additional error to any applied RFID localization method.

TABLE I
EXPERIMENTAL RESULTS FOR PHASE RELOCK

speed	error in 3D space	error in xy plane	error in z coord
5cm/s	44.8cm	16.3cm	39.5cm
10cm/s	50.5cm	18.7cm	41.1cm
20cm/s	69cm	17.1cm	64.1cm
mean	54.86cm	17.37cm	48.25cm

TABLE II
PHASE RELOCK VS GRID-BASED METHODS

method	mean error	std	mean est-time
Phase ReLock	54.86cm	42.1cm	55s
[8], [12]	58.5cm	38.2cm	5.3 hours

Last but most importantly, we have achieved a tremendous improvement of the algorithms speed, as shown in Table II. Whilst the holographic methods required about 5 and half hours to estimate the 3D position of an average of 87 tags, Phase ReLock performed 360 times faster and located the same amount of tags in less than a minute. This reduction-ratio is proportional to the size of the search space, since the speed of Phase ReLock is independent of a calculation's grid, whereas grid-based methods aren't; for a larger and denser grid, that ratio would be further increased.

V. CONCLUSION

In this work, we have presented the 3D extension of "Phase ReLock" [13]; a novel localization method that solves the localization problem via phase unwrapping and non linear optimization. For a localization in the three dimensions, it deploys a robot that moves along non straight trajectories, to reduce the locus of possible tag locations to only two points. Prior information of the half-plane the tags are located in is needed. Experimental results validate the performance of the method. In contrast to related prior-art, it is independent of any grid density and orders of magnitude faster; thus, it can be ideal for a real-time inventorying and localization.

APPENDIX

Let a tag placed at the unknown point $K(x_k, y_k, z_k)$ and an antenna moving along a known line l_1, as shown in Fig. 11. The perpendicular straight-segment l_3 that joins K and l_1 is unique and crosses l_1 at the unique point A. Let R_1 the distance between K and A. For simplicity, x-axis is defined to coincide with line l_1. Consider the vectors $\vec{v_1}$ and $\vec{v_3}$ that are collinear to l_1 and l_3 respectively. Then:

- $\vec{v_1} = (\Delta x_1, 0, 0),\ \Delta x_1 = x_{1,0} - x_1 \neq 0$
- $\vec{v_3} = (x_k - x_1, y_k, z_k)$

We have:

$$\vec{v_1} \perp \vec{v_3} \Rightarrow \vec{v_1} \cdot \vec{v_3} = 0$$

$$\Rightarrow \Delta x_1 (x_k - x_1) = 0 \Rightarrow x_k = x_1 \qquad \text{(a)}$$

$$|\vec{v_3}| = R_1 \Rightarrow \sqrt{(x_k - x_1)^2 + y_k^2 + z_k^2} = R_1 \Rightarrow$$

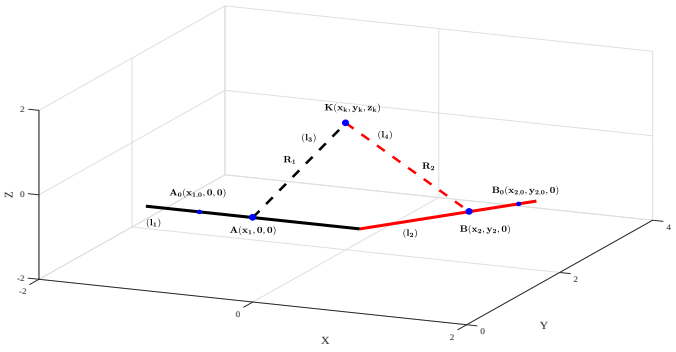

Fig. 11. Geometry of the virtual antenna arrays.

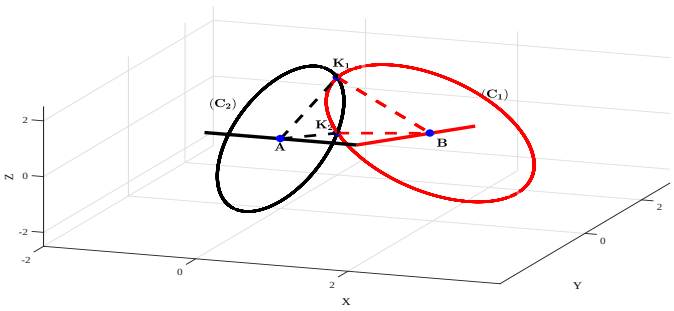

Fig. 12. Tag's location as intersection of the two circular loci.

$$\sqrt{y_k^2 + z_k^2} = R_1 \tag{b}$$

Notice that (b) represents a circle C_1 around l_1, with center A and radius R_1, as shown in Fig. 12. This is in total agreement with subsection III-A and Fig 3, which indicated that in case of a straight path the locus of possible tag locations is a circle around the path.

Let now a second virtual antenna array along the known line l_2, which also lays on plane $z = 0$ (Fig. 11). Similarly, there is a unique straight-segment, denoted as l_4, that joins K and l_2 and is perpendicular to l_2. Let B the unique point of intersection and R_2 the distance between K and B. Lines l_2 and l_4 are represented by the collinear to them vectors, denoted as $\vec{v_2}$ and $\vec{v_4}$ respectively:

- $\vec{v_2} = (\Delta x_2, \Delta y_2, 0),\ \Delta x_2 = x_{2,0} - x_2,\ \Delta y_2 = y_{2,0} - y_2$
- $\vec{v_4} = (x_k - x_2, y_k - y_2, z_k)$

We have:

$$\vec{v_2} \perp \vec{v_4} \Rightarrow \vec{v_2} \cdot \vec{v_4} = 0 \Rightarrow$$

$$\Delta x_2(x_k - x_2) + \Delta y_2(y_k - y_2) = 0 \Rightarrow$$

$$y_k = C, \quad where \quad C = \frac{\Delta y_2 y_2 - \Delta x_2(x_1 - x_2)}{\Delta y_2} \tag{c}$$

$$|\vec{v_4}| = R_2 \Rightarrow \sqrt{(x_k - x_2)^2 + (y_k - y_2)^2 + z_k^2} = R_2 \tag{d}$$

Eq. (d) represents a second circle C_2, with radius R_2 and center B. By substituting (a) and (c) in (d):

$$\sqrt{(x_1 - x_2)^2 + (C - y_2)^2 + z_k^2} = R_2 \Rightarrow$$

$$z_k = \pm D, \quad where \quad D = \left(R_2^2 - (C - y_2)^2 - (x_1 - x_2)^2\right)$$

Notice that x_k and y_k are unique, whilst z_k has 2 symmetrical solutions. Therefore, the unknown position of the tag can be either point K_1 or K_2. K_1 and K_2 are symmetrical in relation to $z = 0$ plane; in general they are symmetrical to the $z = z_i$ plane, where z_i is the antenna's height. Fig. 12 represents points K_1 and K_2 as the intersection of circles C_1 and C_2. Subsequently, the locus of possible tag locations of any additional antenna array at the same plane, would intersect at the same two points.

REFERENCES

[1] RELIEF project, "http://relief.web.auth.gr/?page_id=553lang=en," last accessed on June 5 2019.

[2] A. Almaaitah, K. Ali, H. S. Hassanein, and M. Ibnkahla, "3D passive tag localization schemes for indoor RFID applications," 2010 IEEE International Conference on Communications, pp. 1-5, 2010.

[3] F. Tlili, N. Hamdi, and A. Belghith, "Accurate 3D localization scheme based on active RFID tags for indoor environment," IEEE RFID-TA, 2012, pp. 378-382.

[4] T. Liu, L. Yang, Q. Lin, Y. Guo, and Y. Liu, "Anchor-free backscatter positioning for RFID tags with high accuracy," IEEE INFOCOM, 2014, pp. 379-387.

[5] L.M. Ni,Y. Liu, Y.C. Lau, A.P. Patil, "LANDMARC: indoor location sensing using active RFID," Wireless networks, pp. 701-710, 2004.

[6] Y. Zhao, Y. Liu, and L. M. Ni, "Vire: Active rfid-based localization using virtual reference elimination," Proc. of IEEE ICPP, 2007.

[7] S. Megalou, A. Tzitzis, S. Siachalou, T. Yioultsis, J. Sahalos, E. Tsardoulias, A. Filotheou, A. Symeonidis, L. Petrou, A. Bletsas, and A. G. Dimitriou, "Fingerprinting Localization of RFID tags with Real-Time Performance-Assessment, using a Moving Robot," 13th European conference on Antennas and Propagation, Krakow, Poland, 2019

[8] R. Miesen, F. Kirsch, and M. Vossiek, "UHF RFID localization based on synthetic apertures," IEEE Transactions on Automation Science and Engineering, vol. 10, no. 3, pp. 807-815, 2013.

[9] Y. Zhang, L. Xie, Y. Bu, Y. Wang, J. Wu, and S. Lu, "3-Dimensional Localization via RFID Tag Array," 2017 IEEE 14th International Conference on Mobile Ad Hoc and Sensor Systems, 2017

[10] L. Qiu, Z. Huang, N. Wirstrom, and T. Voigt, "3DinSAR: Object 3D Localization for Indoor RFID Applications," IEEE International Conference on RFID (RFID), 2016.

[11] E. DiGiampaolo, F. Martinelli, "A Robotic System for Localization of Passive UHF-RFID Tagged Objects on Shelves," IEEE Sensors Journal, vol. 18, no. 20, pp. 8558–8568, 2018

[12] A. Motroni, P. Nepa, V. Magnago, A. Buffi, B. Tellini, D. Fontanelli, and D. Macii, "SAR-Based Indoor Localization of UHF-RFID Tags via Mobile Robot," 2018 International Conference on Indoor Positioning and Indoor Navigation (IPIN), Nantes, France, 2018

[13] A. Tzitzis, S. Megalou, S. Siachalou, T. Yioultsis, A. Kehagias, E. Tsardoulias, A. Filotheou, A. Symeonidis, L. Petrou and A. G. Dimitriou, "Phase ReLock - Localization of RFID Tags by a Moving Robot," 13th European conference on Antennas and Propagation, Krakow, Poland, 2019

[14] J. J. More and D. C. Sorensen, "Computing a Trust Region Step," SIAM Journal on Scientific and Statistical Computing, vol. 3, pp. 553-572, 1983.

[15] D. Marquardt, "An Algorithm for Least-Squares Estimation of Nonlinear Parameters," SIAM J. Appl. Math., vol. 11, pp. 431-441, 1963.

[16] K. Levenberg, "A Method for the Solution of Certain Problems in Least Squares," Quart. Appl. Math., vol. 2, pp. 164-168, 1944.

[17] E. Tsardoulias, and L. Petrou, "Critical Rays Scan Match SLAM," Journal of Intelligent & Robotic Systems, vol. 72, no. 3–4, pp. 441–462, 2013